

## **Synthesis, Characterization and Optical properties of PANI/PVA Blends.**

A. F. Mansour, A. Elfalaky\*, and F. Abdel Maged  
Zagazig University, Faculty of Science, Physics Department, Zagazig, Egypt.

---

**Abstract:** Polyaniline was synthesized by the chemical oxidative polymerization of aniline. Poly aniline (PANI) blended with polyvinyl alcohol (PVA) which prepared by solution cast method using N-Methyl Pyrolidone (NMP). The polyaniline powder was characterized by X-ray diffraction (XRD) and scanning electron microscopy (SEM). In this paper we study the optical properties of PANI/PVA blends. Include optical transmission, optical constant, dielectric constants, optical conductivity, and band gaps. This study shows that the absorption increases and transmission decreases as PANI concentration increases in the blend. The extinction coefficient, refractive index, real and imaginary parts and average refractive index values were found to increase with increasing PANI concentration

**Keywords:** PANI, PVA, Blend, XRD, SEM and Optical Properties.

---

### **I. Introduction**

Conducting polymers have recently become an area of wide-spread interest in organic electronics due to their potential application in energy conversion systems such as photovoltaic cells, solar cells, bio sensors etc [1-3]. In view of this, a great deal of interest has been paid to the mechanical, optical and conducting properties of polymers. Polyaniline (PANI) is one of the most useful conducting polymers due to their simple synthesis, good environmental stability. It also has a wide range of electrical properties which can be easily controlled by changing its oxidation and protonation states [4-5]. However, major problems relating to successful utilization of the PANI are poor mechanical property and low solubility in aqueous and organic solvents. Improvement of polyaniline properties can be achieved either by forming composites and nanocomposites of aniline, or blending with commercially available polymers or inorganic material which offers better mechanical and optical properties, stability and process ability of the PANI [6-7]. In the present paper, we report XRD, SEM and optical properties of PANI/ PVA blends.

### **II. Experimental**

#### **2.1 Material**

Aniline Monomer  $C_6H_5NH_2$  (assay 99.5 %) was purchased from central Drug House (P) Ltd. New Delhi-110002 India. Hydrochloric acid (35%AR), Ammonium Hydroxide (30%), Ammonium peroxodisulfate (99% AR) were from Alpha Chemika India.

#### **2.2 Synthesis of Polyaniline (EB)**

Polyaniline was synthesized by polymerization of aniline in the presence of Hydrochloric acid (acts as a catalyst) using ammonium peroxodisulfate (APS) (acts as an oxidizing agent) by chemical oxidative polymerization method.

For the synthesis Ammonium peroxodisulfate,  $(NH_4)_2S_2O_8$  (36.9g), was dissolved in 210 ml of 1M HCl in a 500 ml beaker and kept at 25 °C. Aniline (15g), was dissolved in 225 ml of 1MHCl in another 500 ml beaker and also kept at 25 °C. Then, ammonium peroxodisulfate solution was added slowly to the aniline solution over a period of ~1 minute. The flask was left for 30 minutes, during which the temperature remained constant at 25 °C. The solution started to take on a blue-green tint after one to three minutes, and then became intense blue green with a coppery glint. After 30 minutes, the precipitate was collected on a Büchner funnel and flask using a water aspirator. The precipitate was washed with deionized water until the filtrate became colorless. The liquid level in the filter should be constantly adjusted to be above the top of the precipitate. This prevents cracking of the precipitate and hence avoids inefficient washing of the precipitate. After washing, the precipitate remained under suction for ~10 minutes until significant cracking of the moist filter cake occurred. Afterwards, the partially dried precipitate cake was suspended with constant stirring in 100 ml of  $NH_4OH$  (24%) solution in order to convert the polyaniline hydrochloride (emeraldine salt) to polyaniline (emeraldine base).

The suspended solution was stirred for one hour. The powder was collected on a Büchner funnel and flask using a water aspirator and partially dried under suction for ~10 minutes. The precipitate cake was then washed with 1 liter (100 ml per portion) deionized water. The black cake was partially dried on the funnel under suction for ~30 minutes on completion of the last washing, following by drying under vacuum at 60 °C for 48 hours to give purple powder

### 2.3 Synthesis of PANI / PVA Blends:-

The PANI with different concentrations (0.28%, 0.42%, 0.5% and 1% wt) was dissolved in N-methyl-2-pyrrolidone (NMP) under continuous stirring for 2 hours. PVA was dissolved in distilled water at 70°C under continuous stirring for 3 hours. PANI/PVA films were prepared by casting method from mixed solutions.

## III. Results And Discussion

### 3.1. X-ray diffraction

Figure (1) shows X-ray diffraction pattern of pure polyaniline in the emeraldine base form. It can be noticed that it has amorphous nature with a broad peak centered at  $2\theta = 25.30^\circ$ [8].

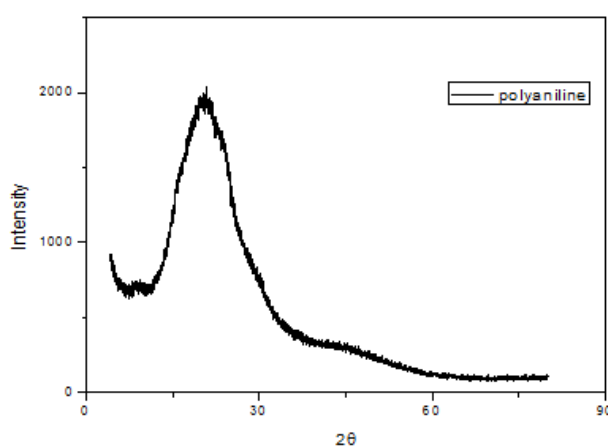


Fig. 1: XRD pattern of PANI powder.

### 3.2. Scanning Electron Microscopy (SEM)

Figure (2) shows SEM micrograph of pure PANI (EB). The SEM photograph shows typical features of the polymer where it is mainly composed of irregularly arranged granular and flakes with sharp edges. Moreover, the structure looks more porous.

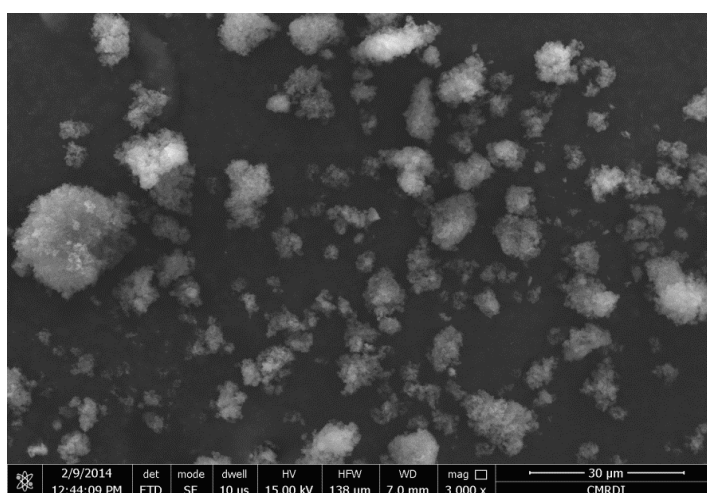


Figure 2: SEM micrograph of polyaniline (EB) powder.

### 3.3 Optical properties

#### 3.3.1 Absorption, transmission and reflection spectra of pure PVA and PANI / PVA blend films.

The UV-VIS absorbance spectra in the region 200-1100 nm for PVA and PANI/ PVA blend are shown in fig. (3-a). The absorption spectrum of pure PVA has absorbance band at 280 nm and shoulder at 330 nm, these bands were assigned to  $\pi-\pi^*$  and  $n-\pi^*$  electronic transitions respectively [9-10]. The absorption spectra of PANI/ PVA of (0.28, 0.42, 0.5 and 1 wt %) show two characteristic absorption peaks attributed to the conducting emeraldine salt. That at 300 nm was assigned to the  $\pi-\pi^*$  transition and the other at about 700 nm is assigned to the polaron band [11]. The absorption increased with increasing PANI concentration. In accordance with Beers law, the absorption is proportional to the number of absorbing molecules. It is clear from the figure that the absorption edges have a red shift with increasing PANI concentrations indicating the decrease in optical band gap for the doped film.

The transmittance spectra of PVA and PANI/PVA films are shown in fig. (3-b). The transmittance spectra for PVA showed nearly 90% transmissions for wavelength greater than 500 nm. The decreasing in transmission with increasing the concentration of PANI in blend, leads to a decrease in light scattering losses. The relationship between the reflectance and wavelength is shown in fig. (3-c). The reflectance increases with increasing the PANI concentration.

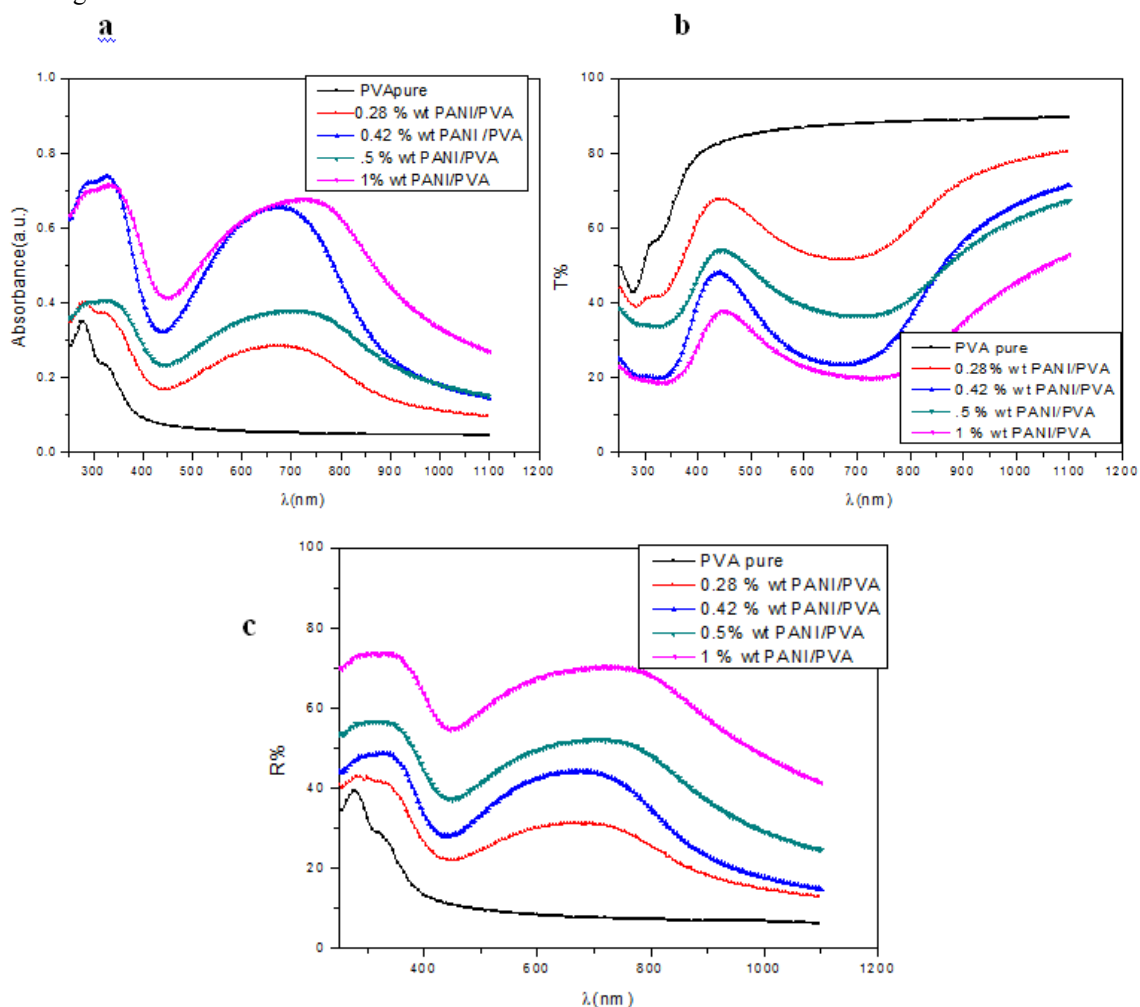


Fig (3) (a) Absorption, (b) transmission and (c) reflectance spectra as a function of wave length for PANI/PVA blend films.

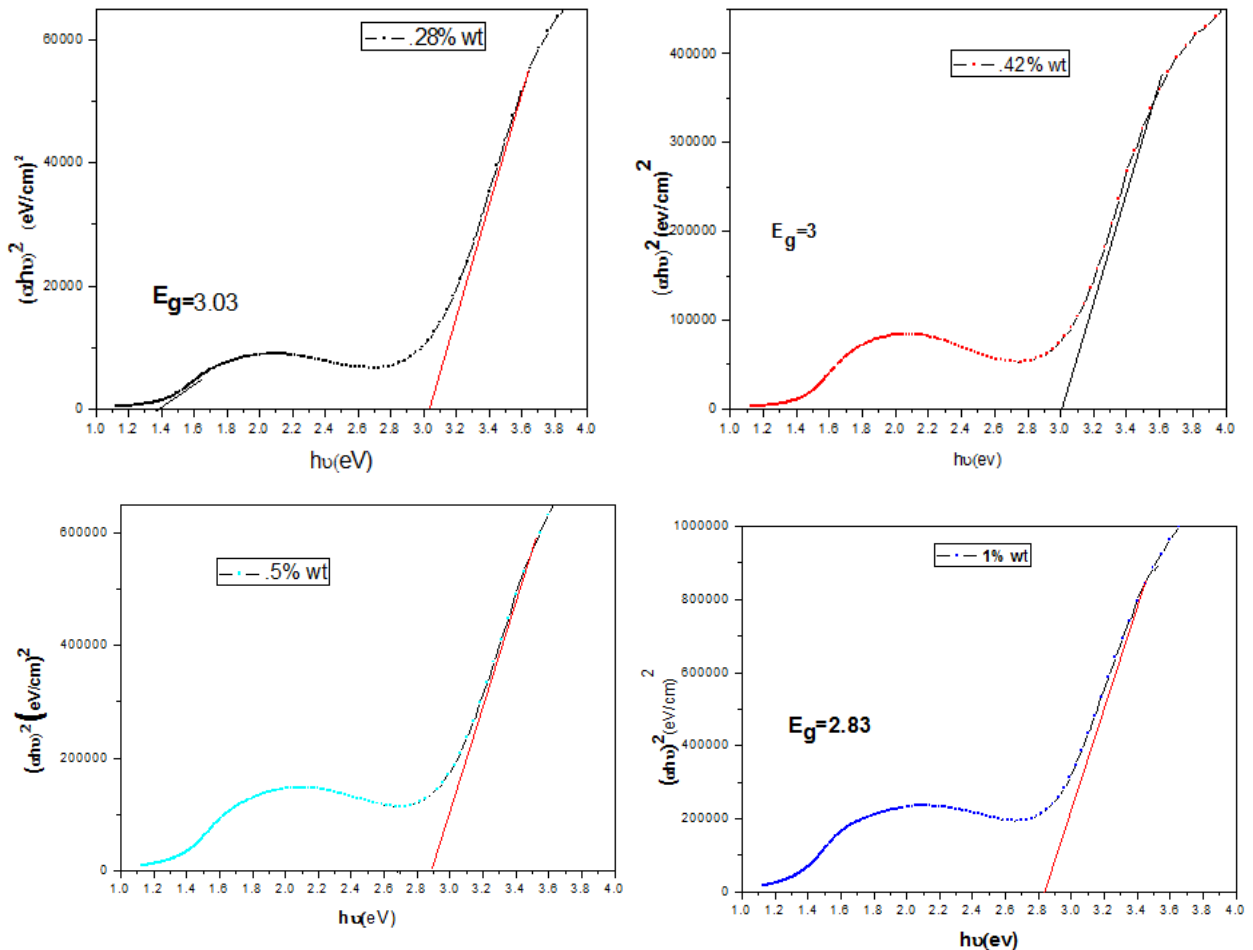
#### 3.3.2 Optical band gap

The optical energy gape ( $E_g$ ) of the films is calculated by [12]:

$$\alpha h\nu = B (h\nu - E_g)^m \quad (1)$$

where  $h\nu$  is the energy of incident photon,  $E_g$  is the optical energy band gap,  $B$  is a constant known as the disorder parameter which is nearly independent of photon energy parameter and  $m$  is the power coefficient with the value that is determined by the type of possible electronic transitions. For the direct and indirect allowed transition  $m=1/2$  or  $2$ , respectively [13].

The best line fit is obtained in the curve of  $m = 1/2$ , which indicates the type of electronic transition is direct allowed transition. The value of optical band gap can be established from figure (4) through extrapolating the linear portion to  $(\alpha h\nu)^2 = 0$ . Table (1) records the optical band gap of PVA and PANI/PVA films. It was observed that the values of energy gap decrease from 3.03 to 2.83 eV with increasing of the weight percentage of PANI, which means a rising in conductivity [14]. The reduction in the optical bandgap is probably due to the modification of the polymer blend [15].



Fig(4) plots of  $(\alpha h\nu)^2$  vs.  $(h\nu)$  for PANI/PVA blend films.

The refractive index ( $n$ ) is a fundamental optical property of polymers that is directly related to other optical, electrical, and magnetic properties, and also of interest to those studying the physical, chemical, and molecular properties of polymers by optical techniques. The optical properties of the samples can be characterized by the complex refractive index. The complex refractive index is expressed as  $n^* = n(\omega) + ik(\omega)$  where  $n$  is the real part and  $k$  is the imaginary part of refractive index. The refractive index,  $n$ , can be determined from the following relation [16]:

$$n = \frac{1+R}{1-R} + \left[ \frac{4R}{(1-R)^2} - K^2 \right]^{1/2} \quad (2)$$

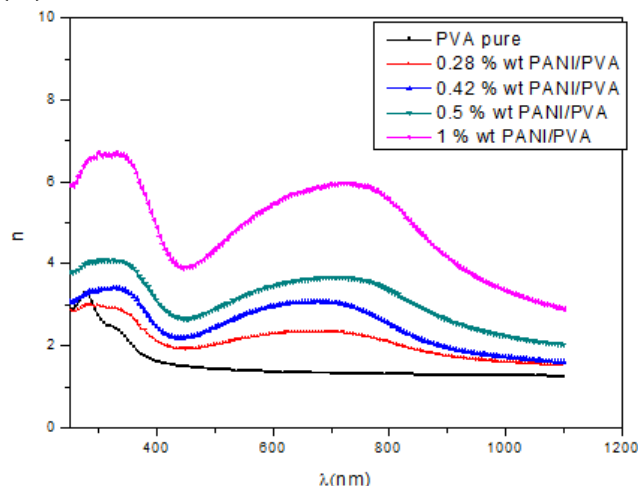
where  $R$  is the reflectivity and  $k$  ( $k = \alpha\lambda / 4\pi$ ) is the extinction coefficient. The extinction coefficient  $k$  describes the properties of the material with respect to light of a given wavelength and indicates the absorption changes when the electromagnetic wave propagates through the material.

Fig. (5) illustrates the values of  $n$  as a function of the wavelength for PVA and PANI/ PVA films. The value of  $n$  increases with increasing of PANI due to the addition of PANI it deportation that is led to decreasing, in general, the reflective index increases by increasing the C – H bonds [17-18]. The relationship between the extinction coefficient ( $k$ ) and wavelength of the films are shown in Figure (6). It can be clearly seen that the extinction coefficient increase as the doping percentage of PANI increased, this may be attributed to high absorption coefficient.

**3.3.4 Dispersion energy, oscillator strength and static refractive index from Wemple-DiDomenico model.**

Wemple and DiDomenico [19-20] have developed a model where the refractive index dispersion is studied in the region of transparency below the gap, using the single-effective oscillator approximation. Defining two parameters, the oscillator energy,  $E_o$  and the dispersion energy  $E_d$ , the single oscillator model below absorption edge is defined as [20]:

$$n^2(\omega)-1 = \frac{E_o E_d}{E_o^2 - (h\omega)^2} \quad (3)$$



**Fig (5) The refractive index of PANI/PVA blend at different concentration of PANI.**

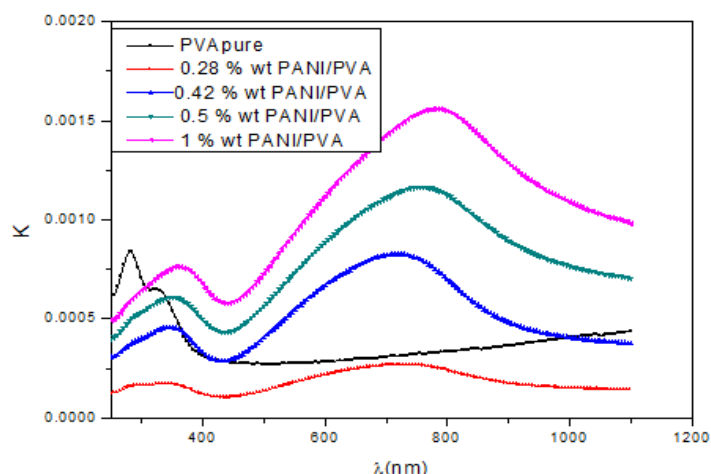


**Fig (6) The extinction coefficient of PANI/PVA blend at different concentration of PANI.**

where  $h$  is the Plank's constant,  $\omega$  is the angular frequency,  $E_o$  is the average excitation energy for electronic transitions or the oscillator energy.  $E_d$  is the dispersion energy which measures the average strength of inter-band optical transitions or the oscillator strength.

By plotting  $(n^2-1)^{-1}$  against  $(h\omega)^2$  and fitting it to straight part of the curve in the low energy region as in fig (7a),  $E_o$  and  $E_d$  are obtained from the slope =  $(E_o E_d)^{-1}$  and intercept =  $E_o/E_d$ . The values of  $E_o$  and  $E_d$  are listed in table (1). The static refractive index  $n_o$  at zero photon energy (long wavelength) evaluated from equation (3), i.e  $n_o^2 = 1 + E_d/E_o$  is also shown in table (1).

**Table (1)optical parameters of PVA and PANI/PVA blend of different concentrations of PANI.**

PANI concentration	$E_o$ (ev)	$E_d$ (ev)	$E_{g1}$ (eV)	$E_{g2}^{op}$ (ev)	$n_o$
0%	4.85	4.06		3.88	1.35
.28 % wt0	1.746	1.33	1.38	3.03	1.32
.42% wt0	1.64	1.38	1.36	3	1.35
.5% wt0	1.6	2.59	1.34	2.9	1.6
1% wt	1.56	5.8	1.3	2.83	7.15

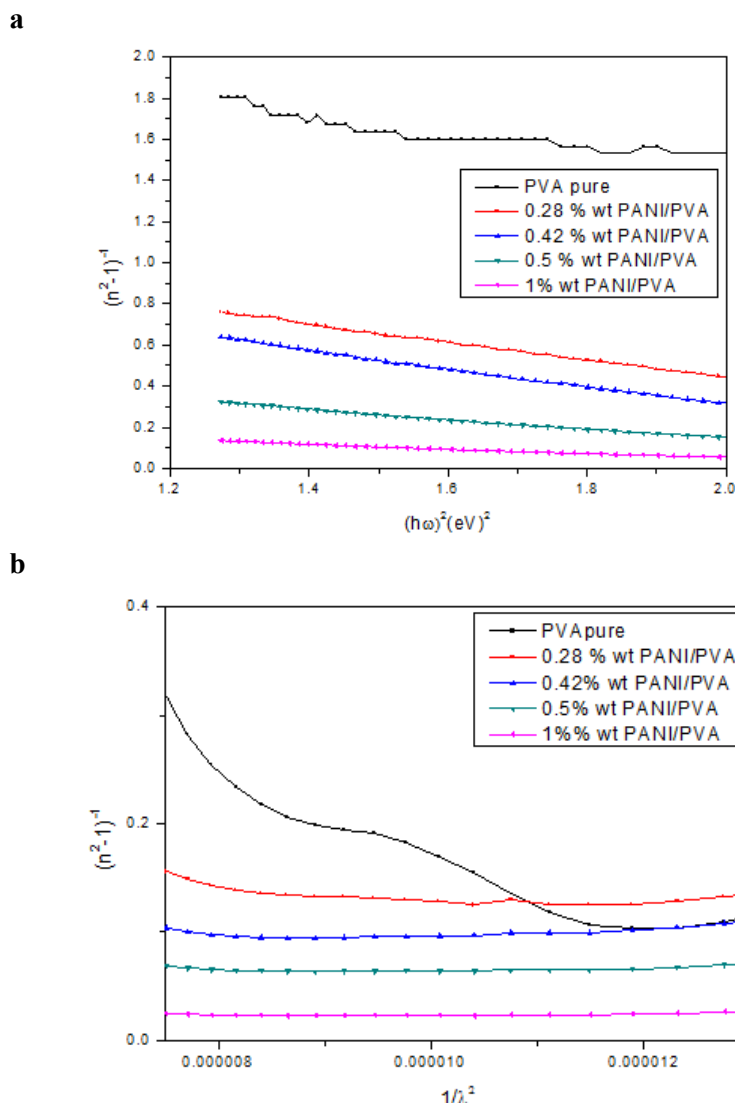


Fig (7) Plots of (a)  $(n^2-1)^{-1}$  vs.  $(h\omega)^2$  (b)  $(n^2-1)^{-1}$  vs.  $(1/\lambda^2)$  for pure PVA and PANI/PVA blends.

The observed decrease in the value of  $E_0$  with increasing PANI concentration can be attributed to the red shift of the optical absorption spectra. The refractive index  $n$  can also be analyzed to determine the long wavelength (low energy) refractive index  $n_0$ , average oscillator wavelength  $\lambda_0$  and oscillator length  $s_0$  of the films. These values can be obtained by using the single Sellmeier oscillator at low energy [16, 21].

$$\frac{n_0^2-1}{n^2-1} = 1 - \left(\frac{\lambda_0}{\lambda}\right)^2 \quad (4)$$

where  $n_0$  is the static refractive index, which provides a good indication on the structure and density of the material and it equal to  $\sqrt{\epsilon_{\infty}}$  (static dielectric constant). Rearranging equation (4) gives

$$(n^2-1)^{-1} = \frac{1}{s_0 \lambda_0^2} - \frac{1}{s_0 \lambda^2} \quad (5)$$

Here  $s_0 = (n_0^2-1) / \lambda_0^2$

The graph between  $(n^2-1)^{-1}$  and  $\lambda^{-2}$  is shown in figure (7b). The value of  $s_0$  and  $\lambda_0$  were obtained from the slope and intercept of straight line in figure (7b). Table (2) lists the obtained values of  $n_0$ ,  $\lambda_0$  and  $s_0$ . From the table, the values of  $n_0$  increased with increasing PANI concentration in the blend. The same behavior was previously reported when doping in PANI [22].

### 3.3.5. Complex dielectric constants

The complex dielectric function is  $\epsilon = \epsilon_r + i \epsilon_i$  where  $\epsilon_r$  is the real part which associated with the term that shows how much it will slow down the speed of light in the material. It can be determined by using the relation [23]

$$\epsilon_r = n^2 - k^2 = \epsilon_{\infty} - \beta \lambda^2 \quad (6)$$

where,

$$\beta = \frac{e^2}{4\pi^2 c^2 \epsilon_0} \frac{N}{m^*} \quad (7)$$

where  $\epsilon_\infty$  is the high frequency dielectric constant,  $m^*$  is the effective mass of the charge carrier,  $e$  is the electronic charge,  $N$  is the free carrier concentration,  $C$  is the velocity of light and  $\epsilon_0$  is the free space dielectric constant. By plotting a relation between  $\epsilon_r$  and  $\lambda^2$ , as shown in fig.(8 a), we can calculate  $\epsilon_\infty$  and  $(N/m^*)$  from the intercept and the slope of the linear portion of the curve. It is noticed that  $(N/m^*)$  increases with increasing PANI concentration in the blend as shown in table (2).  $\epsilon_i$  is the imaginary part of dielectric constant which shows how a dielectric absorbs energy from an electric field due to dipole motion. The imaginary part of dielectric constant was determined by the following relation [23]

$$\epsilon_i = 2nk \quad (8)$$

The real part of dielectric constant is related to the dispersion, and the imaginary part represents the dissipative rate of electromagnetic wave propagation in the medium. The real and imaginary parts of the dielectric constant as a function of wavelength are shown in Figure 8 (b and c) for pure PVA and PANI/PVA blends at different concentration of PANI. It is clear that the variation of  $\epsilon_r$  mainly depends on the values of  $n^2$  as a result of small values of  $k^2$  in comparison with  $n^2$ , while  $\epsilon_i$  mainly depends on the  $k$  values which are related to the variation of absorption coefficient.

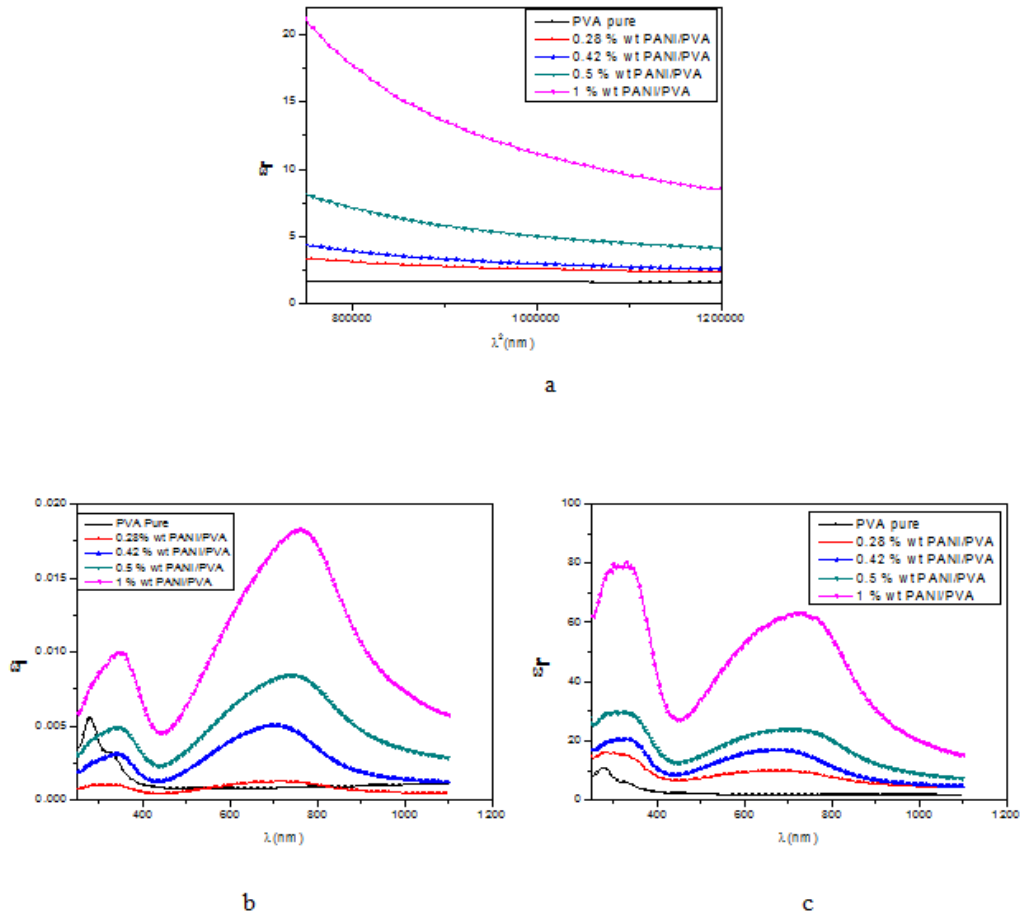


Fig (8) Plots of (a)  $\epsilon_r$  vs.  $\lambda^2$  (b)  $\epsilon_i$  vs.  $\lambda$  and (c)  $\epsilon_r$  vs.  $\lambda$  respectively for PANI/PVA blends of different concentrations of PANI.

Table (2) values of  $\epsilon_{\infty}$ ,  $N/m^*$ ,  $\lambda_0$ ,  $S_0$  and  $W_p$  for PANI/PVA blends.

PANI concentration	$(\epsilon_{\infty})$	$(N/m^*)Kg^{-1}.m^{-3} \times 10^{62}$	$(\lambda_0) \times 10^{-7} m$	$(S_0) \times 10^{12} m^{-2}$	$W_p \times 10^{17} Sec^{-1}$
0%	2.87	0.000023	3.19	8.4	0.026
.28 % wt0	4.6	1.957	7.3	1.4	7.5
.42% wt0	6.45	3.299	7.7	1.36	9.76
.5% wt0	12.8	7.42	7.87	2.5	14.6
1%wt	35.4	2.3	8.14	5.26	81.5

The plasma resonance frequency ( $W_p$ ) of all valence electron involved in the optical transitions was calculated using the following relation [29-30] and reported in table (2).

$$W_p^2 = \frac{e^2 N}{\epsilon_0 m^*} \quad (9)$$

where  $\epsilon_0$  is the dielectric constant of free space ( $8.854 \times 10^{-12}$  F/m). According to this relation, the plasma frequency depends on the concentration of free carriers. The plasma resonance frequency increases with increasing of PANI in the blend.

The optical response of material is mainly studied in terms of the optical conductivity ( $\sigma$ ), which means the electrical conductivity results from the movement of the charge carriers due to alternating electric field of the incident electromagnetic waves. Optical conductivity can be expressed by the following equation [24]:

$$\sigma_{opt} = \frac{anc}{4\pi} \quad (10)$$

An increase was observed in optical conductivity as increasing in doping percentages of PANI as shown in Figure (9). This may be due to increase the contribution of electron transitions between the valence and conduction bands, which lead to reduction of energy gap as a result of sit level generation.

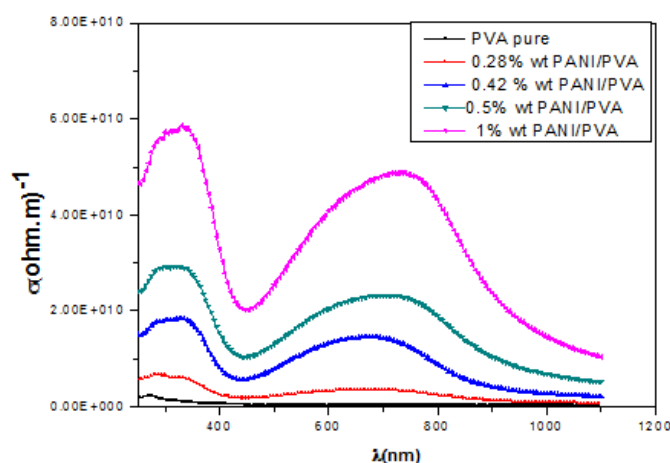


Fig (9) shows the variation of optical conductivity with wavelength for PVA pure and PANI/PVA blend.

#### IV. Conclusion

Polyaniline powder was synthesized by the chemical oxidative polymerization of aniline. X-ray diffraction pattern of pure polyaniline shows that it has amorphous nature with a broad peak centered at  $2\theta = 25.30^\circ$ . The SEM photographs show typical features of the polymer. Measurements of optical energy gap and optical parameters such as refractive index and dielectric constants are strongly dependent of the concentration of PANI in the blends. Optical energy gap value is decreasing from 3.03 eV to 2.83 eV with increasing PANI in blends

#### References

- [1]. J. R. Mac Callum, C. A. Vincent (Eds) Polymer electrolyte rev. Elsevier, Amsterdam. (1987).
- [2]. M. B. Armand, Mater. Sci. 16, 245 (1986)
- [3]. M. A. Ratner, D. F. Shrivar, Chem. Rev. 88, 109 (1988)
- [4]. Vineet Bansal Homabhandari, Mc.Bansal Skldhawan, Indian Journal of pure and Applied Physics, 47, 667 (2009).
- [5]. H. G. Taleghain, M. Aleahmad and H.Eisazadea, World Applied Sciences Journal, 6, 1607 (2009).
- [6]. T. Del Castillo-Castro, M. M. Castillo-Ortega, P. J. Herrera-Franco, D. E. Rodriguez-Felix, Journal of Applied Polymer Science , 119, 2895 (2011).

- [7]. S. C. Raghavendra, Syed Khasim, M. R. Siddappa, M. V. N. Ambika Parasd and A. B. Kulkarni. Bull. Mater.Sci., 26, 733 (2003).
- [8]. A.ElFalaky, A.F. Mansur and F. Abdel-Maged, IOSR-JAP 7, 92 (2015).
- [9]. R. F. Bhajantri, V. Ravindrachary, A. Harisha, V. Crasta, S. P. Nayak, and B. Poojary, Polymer 77, 3591 (2006).
- [10]. A. M. Shehap, Egypt. J. Solids 31, 75 (2008).
- [11]. A. Mirmohseni, G.G. Wallace, Polymer, 44, 3523 (2003).
- [12]. N. F. Mott, E. A. Davis, Electronic Process in Non-crystalline Materials. 2<sup>nd</sup> Edn., Clarendon Press Oxford, UK (1979).
- [13]. J.Tauc, Amorphous and Liquid Semiconductors, Plenum Press, New York (1974).
- [14]. A. Blythe, D. Bloor, Electrical Properties Of Polymers, J. Wiley & Sons, New York, United States of America, (2005).
- [15]. U. S. Sajeev, C. Joseph Mathai, S. Saravanan and R. Rashokan, Bull. Material. Science, 29, 159 (2006).
- [16]. S.Ilican, Y.Caglar, M. Caglar, F. Yakuphanoglu, *J. of Alloys and Comp.*, 480, 234 (2009).
- [17]. W.M. Sayed and L.I. Soliman, Fizika (Zagreb), 4, 147 (2000).
- [18]. I. Kroschwitz, Electronic Properties of Polymers, John Wiley and Sons (1988).
- [19]. M. DiDomenico, S. H.Wemple, J. Appl. Phys., 40, 720 (1969).
- [20]. S. H.Wemple, M. Jr. DiDomenico, Phys. Rev. B 3, 1338 (1971).
- [21]. A. K. Wolaton and T. S. Moss, Proceedings of the Royal Society, 81, 509 (1963).
- [22]. V. Bursikova, P. Sladek, P. Stahel, J. Bursik, Journal of Non-Crystalline Solids 352, 1242 (2006).
- [23]. N. Jamal, M.Sc, thesis, University of Technology in Applied Physics, (2008).
- [24]. A. Mustafa Faisal, Phys. Sci. Res. Int. 1, 1, (2013).